Rotating Rake Mode Measurements Over Passive Treatment in a Ducted Fan

Daniel L. Sutliff
Glenn Research Center, Cleveland, Ohio

NASA STI Program . . . in Profile

Since its founding, NASA has been dedicated to the advancement of aeronautics and space science. The NASA Scientific and Technical Information (STI) program plays a key part in helping NASA maintain this important role.

The NASA STI Program operates under the auspices of the Agency Chief Information Officer. It collects, organizes, provides for archiving, and disseminates NASA's STI. The NASA STI program provides access to the NASA Aeronautics and Space Database and its public interface, the NASA Technical Reports Server, thus providing one of the largest collections of aeronautical and space science STI in the world. Results are published in both non-NASA channels and by NASA in the NASA STI Report Series, which includes the following report types:

- TECHNICAL PUBLICATION. Reports of completed research or a major significant phase of research that present the results of NASA programs and include extensive data or theoretical analysis. Includes compilations of significant scientific and technical data and information deemed to be of continuing reference value. NASA counterpart of peer-reviewed formal professional papers but has less stringent limitations on manuscript length and extent of graphic presentations.

- TECHNICAL MEMORANDUM. Scientific and technical findings that are preliminary or of specialized interest, e.g., quick release reports, working papers, and bibliographies that contain minimal annotation. Does not contain extensive analysis.

- CONTRACTOR REPORT. Scientific and technical findings by NASA-sponsored contractors and grantees.

- CONFERENCE PUBLICATION. Collected papers from scientific and technical conferences, symposia, seminars, or other meetings sponsored or cosponsored by NASA.

- SPECIAL PUBLICATION. Scientific, technical, or historical information from NASA programs, projects, and missions, often concerned with subjects having substantial public interest.

- TECHNICAL TRANSLATION. English-language translations of foreign scientific and technical material pertinent to NASA's mission.

Specialized services also include creating custom thesauri, building customized databases, organizing and publishing research results.

For more information about the NASA STI program, see the following:

- Access the NASA STI program home page at *http://www.sti.nasa.gov*

- E-mail your question via the Internet to *help@sti.nasa.gov*

- Fax your question to the NASA STI Help Desk at 301–621–0134

- Telephone the NASA STI Help Desk at 301–621–0390

- Write to:
  NASA Center for AeroSpace Information (CASI)
  7115 Standard Drive
  Hanover, MD 21076–1320

Rotating Rake Mode Measurements Over Passive Treatment in a Ducted Fan

Daniel L. Sutliff
Glenn Research Center, Cleveland, Ohio

National Aeronautics and
Space Administration

Glenn Research Center
Cleveland, Ohio 44135

December 2006

Rotating Rake Mode Measurements Over
Passive Treatment in a Ducted Fan

Daniel L. Sutliff
National Aeronautics and Space Administration
Glenn Research Center
Cleveland, Ohio 44135

Abstract

The NASA Glenn Research Center's Rotating Rake mode measurement system has been successful in measuring the modal content propagating in hardwall ducts. This paper proposes an extension of the Rotating Rake measurement and analysis technique to treated sections by developing basis functions based on wall impedance boundary conditions for flow conditions (i.e., constant duct area and Mach number) where the closed form analytical solution exists. Analytical equations developed to estimate mode power are incorporated. This method is verified by decomposing and analyzing radial pressure profiles generated numerically by the Eversman propagation code. Several modes, frequencies and impedances are evaluated. Data from a low-speed ducted fan with several different impedance conditions was acquired and reduced to determine the best fit to the data. Using the impedance boundary conditions result in better mode measurement solutions.

Symbol List

A duct area
$\hat{A}$ admittance
C mode normalizing coefficient
c speed of sound
D duct diameter
E duct profile function
f frequency
I acoustic intensity
J Bessel function of the 1st kind
L Length
M Mach number
m circumferential mode index
n temporal mode index
P mode pressure
$\hat{P}$ acoustic power
R duct radius
p pressure
r radial coordinate
t temporal coordinate
U steady velocity
u unsteady velocity
x axial coordinate
Y Bessel function of the second kind
Z normalized acoustic impedance

α   magnitude of eigenvalue
ϕ   phase of eigenvalue
η   reduced frequency
κ   eigenvalue
σ   duct diameter ratio
ρ   density
θ   circumferential coordinate
ζ   cut-off ratio

Introduction

In order to develop fan tone noise reduction concepts, a diagnostic tool was needed to measure the interaction modes of ducted fans. A concept for a continuously rotating microphone rake (ref. 1) was put forth that would be able to obtain all modal amplitudes in a reasonable data acquisition time. The key concept of the Rotating Rake is by slowly rotating locked to the rotor shaft, a Doppler shift is imparted to the duct spinning modes that is uniquely based on the mode physics. The resulting Rotating Rake system developed by the NASA Glenn Research Center (ref. 2) made several advances in the understanding of turbofan mode generation. In addition to directly evaluating a noise reduction technique, this diagnostic tool can provide an experimental database to which the results of aero-acoustic prediction or propagation codes can be benchmarked. The current data analysis for the Rotating Rake system uses closed form analytical solutions that are readily obtained for hardwall, circular ducts with uniform mean flow. For this paper, extended analysis is proposed that will allow the data analysis to include the effects of uniform mean flow in a softwall duct.

Closed Form Analytical Solution

Cylindrical Wave Equation

The propagation of sound in a circular duct with uniform flow is governed by the convective wave equation. In cylindrical coordinates the well-known general solution is:

$$P(\theta,r,x,t) = p_{mnf} * E_{mn}(k_{mn}r)e^{i(2\pi ft + m\theta \pm k_{mn}x)} \qquad \text{where:} \quad E_{mn}(\kappa_{mn}r) = C_{mn}[J_m(\kappa_{mn}r)] \quad (1)$$

is a solution to Bessel's equation. The index m is defined as the circumferential order defining the number of pressure cycles in the circumferential direction. The index n defines the radial order, the number of pressure nodes in the radial direction. The nature of the radial rake indicates that of primary interest is the radial solution. The function E is the form of the radial pressure profile across the duct. The Doppler induced shift of the circumferential modes allows for solution from the Rotating Rake analysis in the radial direction separately.

The constant, C_{mn}, is a weighting factor that normalizes the arbitrary Bessel function profile to a desired physical property. The normalizing physical property chosen for Rotating Rake analysis is:

$$\int_{area} p^2 dA \equiv A \qquad \text{which results in:} \quad \frac{1}{C_{mn}^2} = \frac{\pi}{2}\left(1 - \frac{m^2}{\kappa_{mn}^2}\right)\left[J_m(\kappa_{mn})\right]^2 \qquad (2)$$

For selected physical cases (hardwall condition or no-flow) this result arises from the principle of orthogonally. For the general case, the E-functions based on the eigenvalue solution are not orthogonal.

However the above identity for C_{mn} is used for convenience in these cases; it will have a complex solution.

Eigenvalue Analytical Solution

The eigenvalues are determined from the boundary conditions; in the standard case it is the hardwall condition that the acoustic pressure be normal to the duct outer wall (a consequence of zero acoustic velocity at the wall). For a duct with passive treatment (softwall) the boundary condition is a function of the acoustic admittance (ref. 3):

$$\frac{p}{v} = \frac{Z}{\rho c}; \quad \hat{A} = \frac{\rho c}{Z}; \quad \eta = \frac{\omega R}{c} \tag{3}$$

$$outer\ wall: \quad \kappa_{mn} \frac{E_{m-1,n}(\kappa_{mn})}{E_{mn}(\kappa_{mn})} - m = -i\eta \hat{A} \left(1 - M \frac{k_{mn}}{\eta}\right)^2 \tag{4}$$

Equation (4) can be solved using standard solution techniques. The eigenvalues are then used to determine the eigenfunctions to which the least squares curve fit solution is applied as outlined in reference 2 in a direct fashion. The above boundary conditions show that complex eigenvalues result from the softwall case.

Mode power is an important parameter in duct acoustics and provides a better description of the acoustic field, compared to mode pressure, especially when relating to the external acoustics. Using the equations derived in reference 2 an approximation to power is used for data analysis. This is recognized to be an approximation to the complete answer since the cross terms in the expansion of the power solution is ignored. This approximation of power, and the final form of the computation used is:

$$Power \rightarrow \hat{P} = \int_A \langle I_x \rangle dA; \quad I_x = \left(\frac{p}{\rho_0} + Uu\right)(\rho_0 u + \rho U); \quad \Rightarrow \quad \hat{P} = \mp \frac{\pi R^2 (1-\sigma^2)}{\rho_0 c_0} |\beta|^4 \Re \left\{ \frac{\sqrt{1 - \frac{1}{\zeta^2}}}{\left|1 \pm M\sqrt{1 - \frac{1}{\zeta^2}}\right|^2} \right\} |P|^2 \tag{5}$$

This form mathematically illustrates the effect of cut-off ratio. For the hardwall case the cut-off ratio is a pure real number. If the cut-off ratio is greater than one, then the term in braces is also a real number, hence non-zero power. If the cut-off ratio is less than one, the numerator becomes a pure imaginary number due to the *square* root (the denominator is a magnitude term) and power is identically zero. For the softwall, case the cut-off ratio is a complex number (ref. 4) and non-zero power exists regardless of the cut-off ratio magnitude (power is the real component of the term in the braces).

$$\zeta = \frac{\pi f D}{\alpha \sqrt{(1-M^2)\cos(2\phi)}}; \quad k = \alpha e^{i\phi} \tag{6}$$

Hardwall: (ζ real):   (i) $\zeta < 1$; $\Re\{bi\}$; $\hat{P} = 0$ Softwall: (ζ complex):   (i) $|\zeta| < 1$; $\Re\{a+bi\}$; $\hat{P} \neq 0$ (7)
                (ii) $\zeta > 1$; $\Re\{a\}$; $\hat{P} \neq 0$ (ii) $|\zeta| > 1$; $\Re\{a+bi\}$; $\hat{P} \neq 0$

The analysis described above for processing the data obtained from the Rotating Rake system shows that the measured acoustic pressure field is easily decomposed into a series of radial mode functions for each complex circumferential mode obtained from Fourier analysis of the Rake microphone signals. These radial mode functions are formed from a weighted sum of Bessel functions that are a closed formed solution to the governing wave equation in a circular or annular duct for the following conditions: (a) the walls of the duct are hard and there is no mean flow, (b) the walls of the duct are hard and there is a uniform mean flow, and (c) the walls of the duct are lined with a locally reacting impedance and there is no mean flow. For these cases, the orthogonal properties of the Bessel functions allow the complex amplitudes of the radial modes to be easily obtained from an integration of the pressure disturbance across the area of the duct. In addition, there is a closed form relation between the radial eigenvalues that are part of the argument of the Bessel functions and the axial wave number, which determines the propagation and/or decay of the mode in the axial direction of the duct.

Results and Discussion

To determine the modal solution using the analytically derived eigenvalues, a plane of assumed impedances was used in the Rotating Rake solution, and the eigenfunctions obtained from that assumed impedance were used to generate the least square fit to the data. The assumption is made that solution resulting in the minimum error to the least-squares fit is the impedance.

Eversman Analytical Solution

The Eversman Inlet Radiation (ref. 5) code was used to investigate the details of a mode profile over a treated section in a cylindrical duct. A grid model used for earlier experimental verification (ref. 6) of the Eversman code was modified to incorporate a treated section of the duct wall is shown in figure 1. The treated section impedance and length were varied in several runs. The optimum impedance based on the geometry and input modal content was determined (ref. 7) ($Z_{opt} = 0.67–0.17i$). The near optimum and several non-optimum cases were run. Circumferential mode 2 (hardwall profile) was chosen and input at the source plane; a fixed value for all runs. The magnitude and phase of the radial pressure at a selected axial location inside the duct were extracted from the code solution. Mach number effects were also investigated.
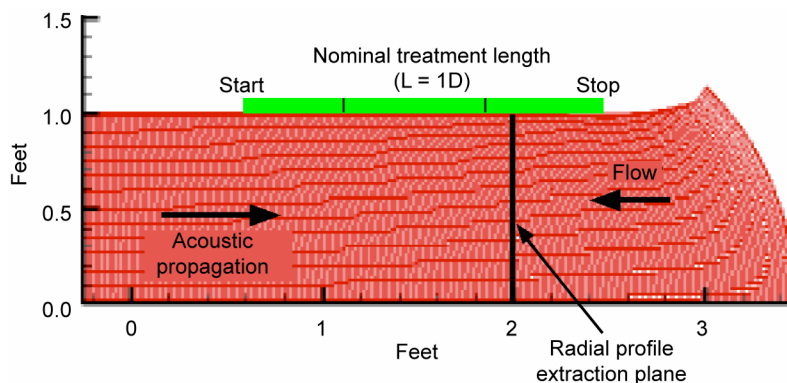

Figure 1.—Grid used in Eversman analytical solutions showing extent of treatment.

TABLE I.—MODE AMPLITUDES SOLUTIONS

```
         Hub-to-Tip ratio = 0.0    Corrected RPM = 1200    Duct Mach# = 0.000
         BPF Harmonic = 1    Circumferential Mode = 2    Radial Mode (max) = 1


         (a)  Case HW / Processed with HW
         Radial    Mag   Phase     Cut-off-real/imag      Decay    Power
           0      142.6   34.1       1.179   0.000          0.0    140.3
           1       76.8   51.1       0.537   0.000         24.6      0.0
         Avg Vector Error = 0.02%              Total Circum Mode Power = 140.3


         (b) Case  Z = 2.16-2.88i / Processed with HW eigenvalues
         Radial    Mag   Phase     Cut-off-real/imag      Decay    Power
           0      132.6   36.5       1.179   0.000          0.0    130.3
           1      108.1 -175.5       0.537   0.000         24.6      0.0
         Avg Vector Error = 2.64%              Total Circum Mode Power = 130.3


         (c) Case  Z = 0.60-0.20i / Processed with HW eigenvalues
         Radial    Mag   Phase     Cut-off-real/imag      Decay    Power
           0       89.1  110.6       1.179   0.000          0.0     86.8
           1       85.4 -158.8       0.537   0.000         24.6      0.0
         Avg Vector Error = 19.32%             Total Circum Mode Power =  86.8
```

Table I shows the error for three different conditions. The duct parameters are shown in the header. The standard fit to a mode in a hardwall duct is shown in table I(a). The least squares fit using the eigenfunctions based on the well-known hardwall eigenvalues is nearly zero. The power remains in the input (2,0) mode. Table I (case b) the pressure profile extracted from a case with non-optimum impedance ($Z = 2.16$–$2.88i$) is reduced using the hardwall (HW) eigenvalues is shown. This curve fit is still reasonable with ~2.6 percent error in the fit. In table I (case c) the results from a case with near-optimum impedance ($Z = 0.6$–$0.2i$) reduced using the HW eigenvalues is shown. (Being near optimum, the attenuation is significant but the numerical solution is still valid). This curve fit is, not surprisingly, poor with a 19 percent error.

Insight into this result can be gained by using the impedances to compute the eigenvalues and eigenfunctions. The resulting mode shapes (eigenfunctions) are shown in figure 2(a) for the first 3 radial modes of m-order 2. Figure 2(b) shows the same modal profiles normalized by the constant C_{mn} which has the effect of forcing the area under the curve to be constant and referencing the phase at $r = 1$. The distinct radial magnitude crossings and the 180° phase shifts of the hardwall modes are obvious in part (i). For an impedance well off optimum (ii) the magnitude of the radial profile is still distinctly apparent, but the phase shifts are no longer exactly 180°. In figure (3) the profiles now take on a significantly non-hardwall appearance. The magnitude of the profile of the zeroth radial is taking on characteristics of a higher order mode. The phase of the radial profile is not necessarily distinct in terms of radial mode phase shifting, especially concerning the zeroth and first radials. Indeed it is difficult to distinguish mode orders (ref. 8). This becomes more difficult as the optimum impedance is approached. This phenomenon has been noted and identified as 'surface acoustic waves' (ref. 9) and the 'double-eigenvalue' (ref. 10) in earlier papers.

The same radial profile data is reprocessed using the appropriate eigenvalues to determine the eigenfunctions used in the least squares fit solution and the results shown in table II. It can be seen that the fit error is reduced significantly. Figure 3(a) shows the error in the curve fit and the computed power levels as a function of impedance. It can be seen that the minimum error is at the actual impedance. This error plane gradient is extremely shallow, indeed essentially flat. Also, note the computation of the power depends upon the impedance (by way of the cut-off ratio) as in equations (5) and (6). At this non-optimum impedance the power changes very little as the impedance changes. The implication being that an iterative solution to find the actual impedance (if it were unknown) would have difficulty converging to a minimum if any experimental error were present, however since the power sensitivity to changing impedance is low in this regime, the "tolerance" in the desired impedance determination may be high.
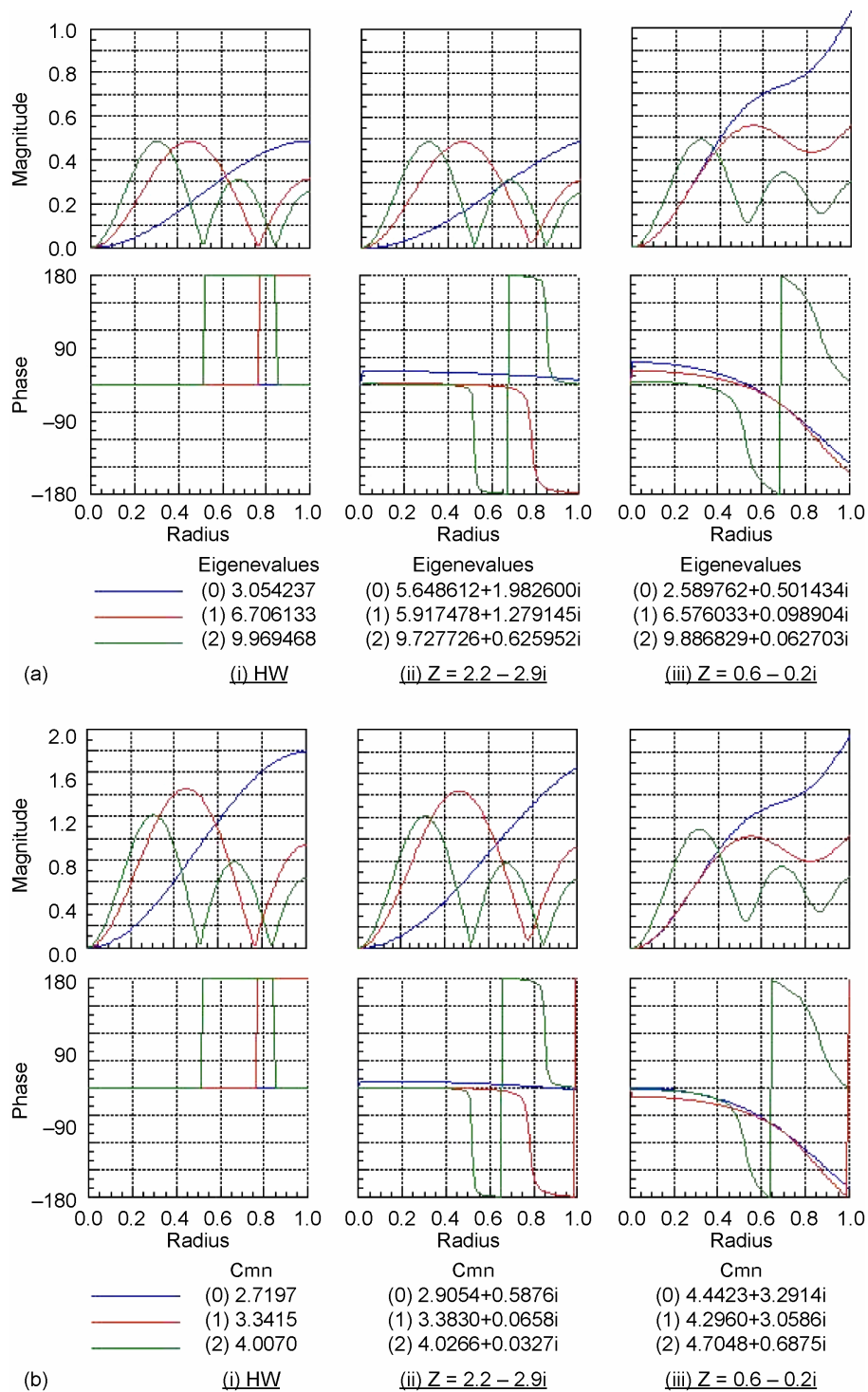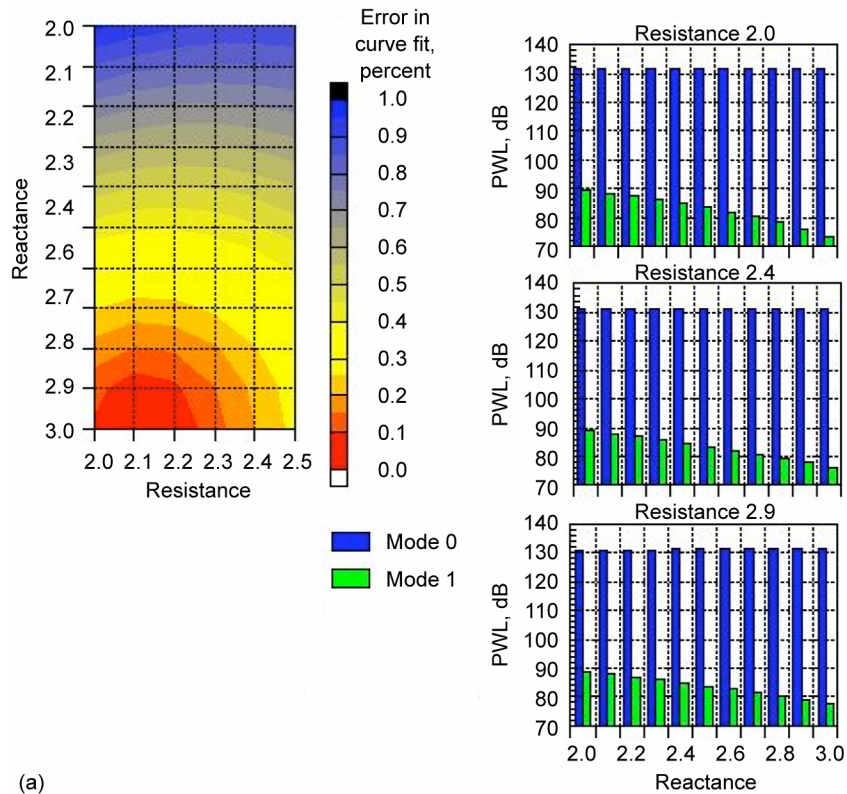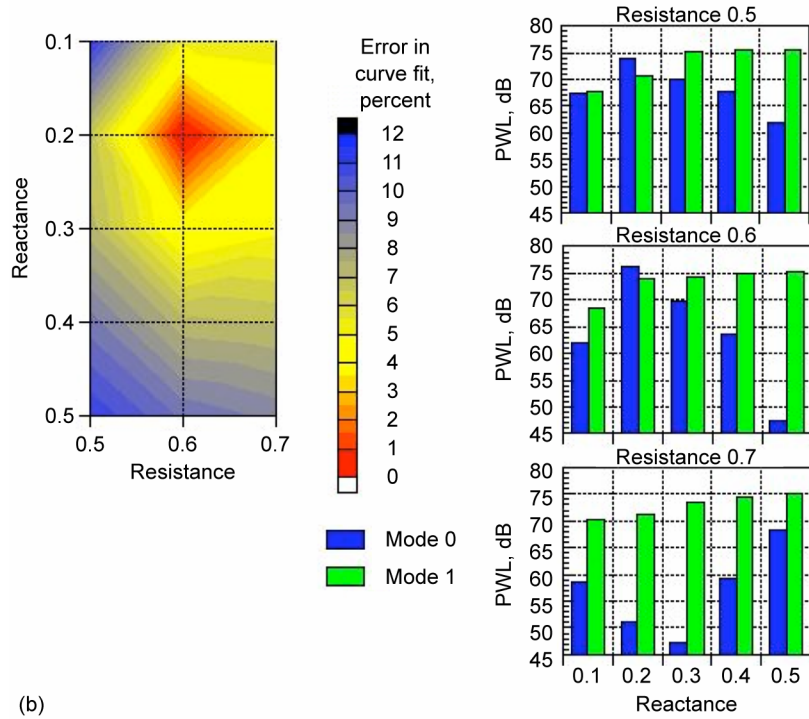
Figure 2.—(2, n) Eigenfunctions. (a) Un-Normalized. (b) Normalized.

Figure 3. Effect on the error and PWL. (a) Z = 2.16-2.88i (off-optimim).
(b) Z = 0.6-0.2i (near-optimim).

TABLE II.—MODE AMPLITUDES SOLUTIONS FOR ACTUAL IMPEDANCE

```
Hub-to-Tip ratio = 0.0   Corrected RPM = 1200    Duct Mach# = 0.000
BPF Harmonic = 1    Circumferential Mode = 2    Radial Mode (max) = 1
```

(a) Case Z = 2.16-2.88i / Processed with Z = 2.16-2.88i eigenvalues

Radial	Mag	Phase	Cut-off-real/imag		Decay	Power
0	132.4	15.6	1.340	-0.259	-2.2	131.5
1	90.8	-54.5	0.547	-0.008	-23.9	76.5

Avg Vector Error = 0.09%   Total Circum Mode Power = 131.5

(b) Case Z = 0.60-0.20i / Processed with z = 0.60-0.20i eigenvalues

Radial	Mag	Phase	Cut-off-real/imag		Decay	Power
0	77.5	162.7	0.567	-0.199	-19.9	76.3
1	77.0	81.7	0.581	-0.126	-20.8	73.9

Avg Vector Error = 0.15%   Total Circum Mode Power = 78.3

TABLE III.—EFFECT OF TREATMENT LENGTH

```
Hub-to-Tip ratio = 0.0   Corrected RPM = 1200    Duct Mach# = 0.000
BPF Harmonic = 1    Circumferential Mode = 2   Radial Mode (max) = 1
Z = 0.60-0.20i / Processed with  z = 0.60-0.20i eigenvalues
```

(a) Case for L = 1.0D

Radial	Mag	Phase	Cut-off-real/imag		Decay	Power
0	77.5	162.7	0.567	-0.199	-19.9	76.3
1	77.0	81.7	0.581	-0.126	-20.8	73.9

Avg Vector Error = 0.15%   Total Circum Mode Power = 78.3

(b) Case for L 0.667D

Radial	Mag	Phase	Cut-off-real/imag		Decay	Power
0	102.4	-178.9	0.567	-0.199	-19.9	101.3
1	102.7	65.6	0.581	-0.126	-20.8	99.6

Avg Vector Error = 1.55%   Total Circum Mode Power = 103.5

(c) Case for L 0.333D

Radial	Mag	Phase	Cut-off-real/imag		Decay	Power
0	127.4	-157.0	0.567	-0.199	-19.9	126.3
1	129.5	54.3	0.581	-0.126	-20.8	126.5

Avg Vector Error = 4.18%   Total Circum Mode Power = 129.4

Table II(b) shows the solution for the near-optimum impedance case. Figure 3(b) shows that the gradient of the error with respect to the impedance is very steep. The minimum error occurs at the known impedance, as expected. The power level as a function of impedance is variable. It appears as if an iterative solution would work very well to find an unknown impedance. Furthermore, the variation in computed power level indicates that it would be important to determine the impedance accurately.

Table III shows the effect of treatment length on the accuracy of the solution. The original treatment length was L/D = 1.0; two additional cases, 0.667D and 0.333D are shown. In these cases the end of the treatment was kept fixed, as well as the plane where the radial profile was extracted was kept fixed. The treatment length was reduced by adjusting the starting point (fig. 1) in the duct, leaving the termination and measurement locations the same. As the treatment is shortened, the error increases. This is because the pressure profile propagates along a helical path and it takes a finite distance for the entire profile to propagate "into" and be affected by the treatment.

The effect of higher frequency as well as multiple radial modes input at the source plane are shown in table IV. The higher frequency (a) effectively follows the pattern in reducing L/D, since the higher cut-on ratio of the higher frequency propagates at a more axial direction and requires a greater L/D to become fully modified by the treatment. Adding more radials (b) in the initial source has no effect in the ability of the solution to fit the softwall modes.

Equation (4) shows that the determination of the softwall mode shapes is a function of Mach number. Eversman cases were run with a uniform duct Mach number (table V (a) to (c): –0.115, and (d) to (f): –0.5). As before, attempting to fit the hardwall modes (a) to the pressure profile results in a large error.

TABLE IV.—EFFECT OF HIGHER FREQUENCY AND MULTIPLE RADIALS

Hub-to-Tip ratio = 0.0   Corrected RPM = 1200   Duct Mach# = 0.000
BPF Harmonic = 2   Circumferential Mode = 2   Radial Mode (max) = 2

(a) Case Z = 0.60-0.20i / mode (2,0) input only

Radial	Mag	Phase	Cut-off-real/imag		Decay	Power
0	133.8	-13.9	2.357	0.000	0.0	133.9
1	130.9	16.5	1.074	0.000	0.0	127.0
2	117.8	-166.1	0.722	0.000	30.0	0.0

Avg Vector Error% = 6.49   Total Circum Mode Power = 134.7

Radial	Mag	Phase	Cut-off-real/imag		Decay	Power
0	132.1	-3.0	1.352	-0.118	-2.1	131.0
1	104.1	-154.8	0.812	-0.077	-22.5	97.6
2	90.7	10.0	0.578	-0.214	-38.2	89.7

Avg Vector Error = 0.25%   Total Circum Mode Power = 131.0

(b) Case Z = 0.60-0.20i / mode (2,0), (2,1), (2,2) input

Radial	Mag	Phase	Cut-off-real/imag		Decay	Power
0	129.0	-22.7	1.352	-0.118	-2.1	127.9
1	101.2	-175.3	0.812	-0.077	-22.5	94.6
2	87.7	-9.8	0.578	-0.214	-38.2	86.6

Avg Vector Error = 0.25%   Total Circum Mode Power = 127.9

TABLE V.—EFFECT OF MACH NUMBER

Hub-to-Tip ratio = 0.0   Corrected RPM = 1200   Duct Mach# = vary
BPF Harmonic = 1   Circumferential Mode = 2   Radial Mode (max) = 1

(a) Duct Mach # = -0.115; HW w/ M=0 eigenvalues

Radial	Mag	Phase	Cut-off-real/imag		Decay	Power
0	97.8	-137.4	1.187	0.000	0.0	95.0
1	89.3	2.1	0.540	0.000	24.5	0.0

Avg Vector Error = 15.51%   Total Circum Mode Power = 95.0

(b) Duct Mach # = -0.115; 0.6-0.8i w/ M=0 eigenvalues

Radial	Mag	Phase	Cut-off-real/imag		Decay	Power
0	87.8	151.9	0.604	-0.682	-8.0	87.8
1	80.5	-20.7	0.582	-0.030	-21.9	71.0

Avg Vector Error = 5.98%   Total Circum Mode Power = 87.9

(c) Duct Mach # = -0.115; 0.6-0.8i w/ M=0.115 eigenvalues

Radial	Mag	Phase	Cut-off-real/imag		Decay	Power
0	63.4	-149.4	0.498	-0.465	-13.4	63.6
1	58.8	-14.6	0.576	-0.049	-22.2	51.5

Avg Vector Error = 1.12%   Total Circum Mode Power = 63.8

(d) Duct Mach # = 0.5; HW w/ M=0 eigenvalues

Radial	Mag	Phase	Cut-off-real/imag		Decay	Power
0	86.3	-156.0	1.361	0.000	0.0	80.1
1	83.6	-102.6	0.620	0.000	22.9	0.0

Avg Vector Error = 14.48%   Total Circum Mode Power = 80.1

(e) Duct Mach # = 0.5; 0.6-0.8i w/ M=0 eigenvalues

Radial	Mag	Phase	Cut-off-real/imag		Decay	Power
0	73.0	138.4	0.693	-0.783	-7.3	67.5
1	84.3	-130.8	0.668	-0.034	-20.1	70.9

Avg Vector Error = 11.64%   Total Circum Mode Power = 72.6

(f) Duct Mach # = 0.5; 0.6-0.8i w/ M=0.5 eigenvalues

Radial	Mag	Phase	Cut-off-real/imag		Decay	Power
0	70.0	-153.4	0.778	-0.092	-14.5	60.3
1	72.3	59.4	0.994	-0.000	-2.0	0.0

Avg Vector Error = 1.69%   Total Circum Mode Power = 60.3

Fitting to the softwall modes, but not accounting for the effect of Mach number (b) improves the fit, but the resulting error is still high. Only by accounting for Mach number (c) does the solution fit very well. This effect is more pronounced for higher Mach number (d) through (f).

Experimental Verification

The NASA Glenn Research Center's Advanced Noise Control Fan (ANCF) (ref. 11) was used a test bed to experimentally validate the methodology. The ANCF is a 4-ft diameter low-speed ducted fan. The rotor tip speed is 425 ft/sec at the nominal rotational speed of 1800 rpm. The ANCF has the unique capability to run a variety of rotor-stator combinations to generate desired modes. Figure 4 shows a schematic of the ANCF.

Two linear single-degree-of-freedom (SDOF) liners with a screen mesh on a 34 percent POA perforate were used in these experiments. The normalized design resistance for the two liners is 1.0 ρc and 1.7 ρc. The liner core depth is 1.0 and 0.85 in.; resonance frequencies are 2872 and 3221 Hz, respectively. The 1.0 ρc liner was also ran with 'ρu' tape over the liner to increase the resistance of the liner by an estimated +1.0 ρc. Figure 5 shows the Rotating Rake in the measurement location extending over the liner. Fan speeds of 1400 to 1800 rpm were run with 14 stator vanes. The data were acquired using the standard Rotating Rake acquisition procedure (ref. 12) and decomposed into circumferential modes. The circumferential modes were decomposed into radial modes using the eigenvalues and eigenfunctions determined based on impedance from equation (4). These solutions were analyzed to determine the impedance resulting in the minimum least-square fit error. The resulting impedance is shown in figure 6(a) (for the 1.0 ρc liner) and 6(b) (for the 1.7 ρc liner).
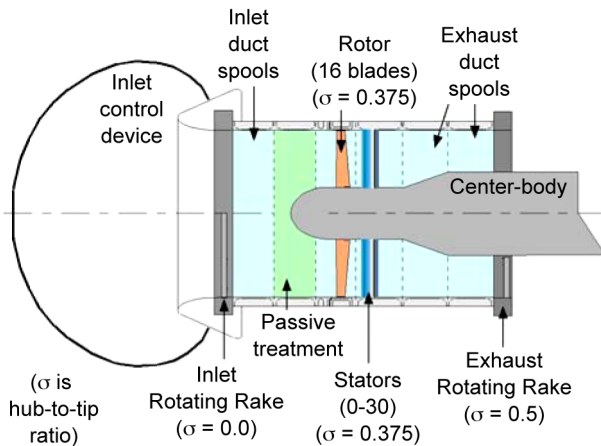

Figure 4.—Schematic of ANCF test ring.

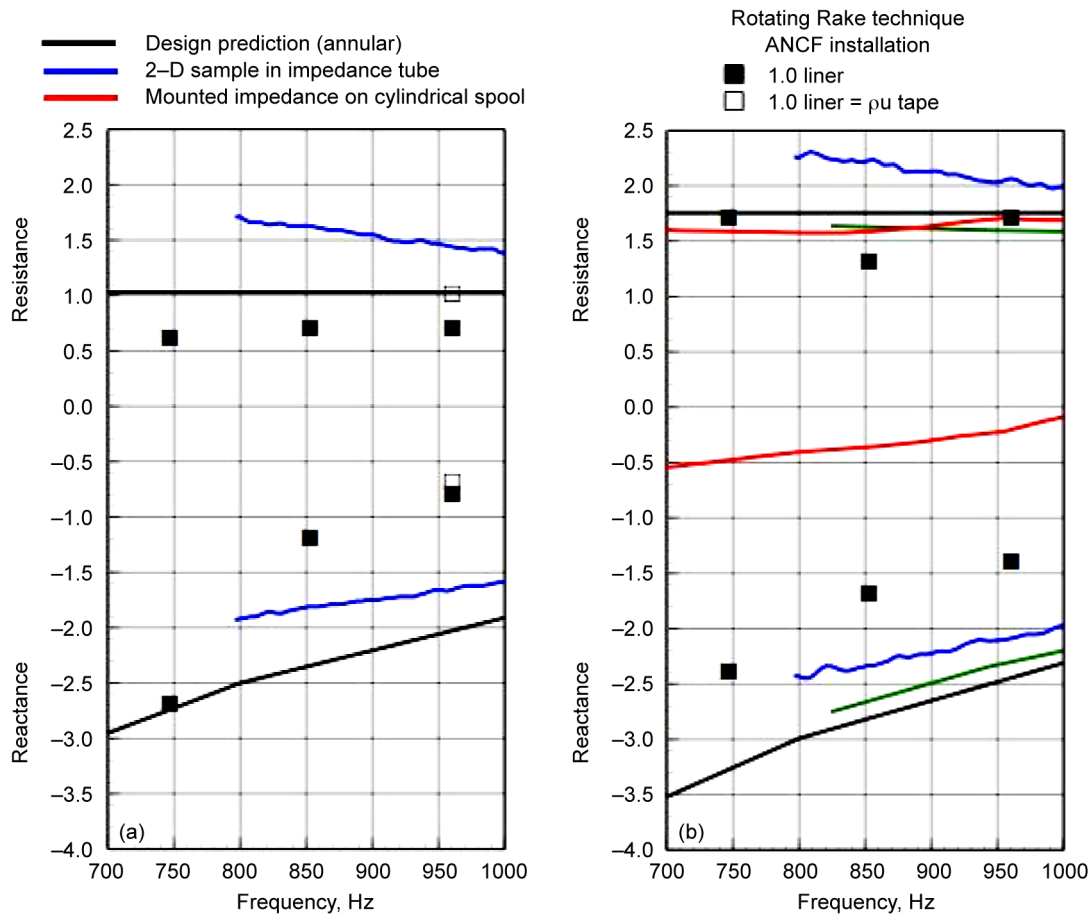Figure 5.—Rotating Rake over liner.

Figure 6.—Experimental data. (a) 1.0 liner design. (b) 1.7 liner design.

Conclusion

A range of conditions (impedance, radial order, cut-off ratio, Mach number, and treatment L/D) were analytically run using the Eversman Inlet propagation code to provide a database to evaluate the effectiveness of the Rotating Rake in measuring the modal characteristics of the acoustic pressure profile over a treated inlet section. A closed-form analytical technique to determine the eigenfunctions that define the mode profile were evaluated and approximations to the mode power were calculated.

The analytical technique was able to decompose the modal structure when the appropriate impedance boundary conditions were incorporated in determining the modes to fit (eigenvalues). Using the appropriate boundary condition was shown to be necessary rather than trying to fit to the standard hard wall modal shapes. For conditions near optimum impedance, the possibility of using an iterative technique is good. The technique can be used to better investigate and understand duct mode propagation in complex environments.

Future Work

Rotating rake data from a full-scale production fan has been acquired with hardwall and softwall inlet. This data will be analyzed to determine the robustness in real applications of the analytical methods presented in this paper. Extending the analysis to annular ducts in order to address treated exhaust ducts is planned. A further extension to the analytical technique required for continued real applications is

applications to treated duct sections with shear flow, that can only be accomplished using the numerical technique is sheared duct flow. Comparisons will be made in the cases were common assumptions between the analytical and the numerical solution hold.

References

1. Cicon, D.E., Sofrin, T.G., and Mathews. D.E., "Investigation of a Continuously Traversing Microphone System for Mode Measurement," NASA CR–168040, PWA–5846–26, November 1982.
2. Sutliff, D.L., "Rotating Rake Mode Measurement System," NASA/TM—2005-213828.
3. Hubbard, H., "Aeroacoustics of Flight Vehicles: Theory and Practice—Volume 2: Noise Control," NASA RP 1258, Vol. 2, WRDC Technical Report 90–3052.
4. Rice, E.J., "Optimum Wall Impedance for Spinning Modes—A Correlation with Mode Cut-off Ratio," Journal of Aircraft, Vol. 16, No. 5.
5. Topol, D.A. and Eversman, E., "TFaNS—Tone Fan Noise Design/Prediction System," NASA/CR—1999-208883, PWA 6420–102.
6. Heidelberg, L.J., Hall, D.G., Bridges, J.E., and Nallasamy, M, "A Unique Ducted Fan Test Bed for Active Noise Control and Aeroacoustic Research," NASA TM–107213, AIAA–96–1740.
7. Rice, E.J., "Spinning Mode Sound Propagation in Ducts with Acoustic Treatment," NASA TN D–7913.
8. Montetaguard, F. and Batard, H., "About the Complexity of Propagation and Radiation of Ducted Modes," AIAA–2000–1955.
9. Vilenski, G., and Rienstra, S.W., "Acoustic Modes in A Ducted Shear Flow," AIAA–2005–3024.
10. Zorumski, W.E. and Mason, J.P. "Multiple Eigenvalues of Sound-Absorbing Circular and Annular Ducts," Journal of the Acoustical Society of America, Vol. 55, No. 6.
11. Loew, R.A., Lauer, J.T., McAllister, J, "The Advanced Noise Control Fan," AIAA–2006–3150.

REPORT DOCUMENTATION PAGE

Form Approved
OMB No. 0704-0188

1. AGENCY USE ONLY *(Leave blank)*	2. REPORT DATE December 2006	3. REPORT TYPE AND DATES COVERED Technical Memorandum

4. TITLE AND SUBTITLE

Rotating Rake Mode Measurements Over Passive Treatment in a Ducted Fan

5. FUNDING NUMBERS

WBS 561581.02.08.03.18.03

6. AUTHOR(S)

Daniel L. Sutliff

7. PERFORMING ORGANIZATION NAME(S) AND ADDRESS(ES)

National Aeronautics and Space Administration
John H. Glenn Research Center at Lewis Field
Cleveland, Ohio 44135–3191

8. PERFORMING ORGANIZATION REPORT NUMBER

E–15785

9. SPONSORING/MONITORING AGENCY NAME(S) AND ADDRESS(ES)

National Aeronautics and Space Administration
Washington, DC 20546–0001

10. SPONSORING/MONITORING AGENCY REPORT NUMBER

NASA TM—2006-214493

11. SUPPLEMENTARY NOTES

Prepared for the 35th International Congress and Exposition on Noise Control Engineering (INTER–NOISE 2006) sponsored by the International Institute of Noise Control Engineering, Honolulu, Hawaii, December 3–6, 2006. Responsible, Daniel L. Sutliff, organization code RTA, 216–433–6290.

12a. DISTRIBUTION/AVAILABILITY STATEMENT

Unclassified - Unlimited
Subject Categories: 07 and 71

Available electronically at http://gltrs.grc.nasa.gov
This publication is available from the NASA Center for AeroSpace Information, 301–621–0390.

12b. DISTRIBUTION CODE

13. ABSTRACT *(Maximum 200 words)*

The NASA Glenn Research Center's Rotating Rake mode measurement system has been successful in measuring the modal content propagating in hardwall ducts. This paper proposes an extension of the Rotating Rake measurement and analysis technique to treated sections by developing basis functions based on wall impedance boundary conditions for flow conditions (i.e., constant duct area and Mach number) where the closed form analytical solution exists. Analytical equations developed to estimate mode power are incorporated. This method is verified by decomposing and analyzing radial pressure profiles generated numerically by the Eversman propagation code. Several modes, frequencies and impedances are evaluated. Data from a low-speed ducted fan with several different impedance conditions was acquired and reduced to determine the best fit to the data. Using the impedance boundary conditions result in better mode measurement solutions.

14. SUBJECT TERMS

Aeroacoustics; Liners; Ducted fans

15. NUMBER OF PAGES

18

16. PRICE CODE

17. SECURITY CLASSIFICATION OF REPORT Unclassified	18. SECURITY CLASSIFICATION OF THIS PAGE Unclassified	19. SECURITY CLASSIFICATION OF ABSTRACT Unclassified	20. LIMITATION OF ABSTRACT